AIP | Journal of Applied Physics

Formation mechanisms of ZnO amorphous layers due to thermal treatment of ZnO thin films grown on pInP (100) substrates

J. M. Yuk, J. Y. Lee, Y. S. No, T. W. Kim, and W. K. Choi

Citation: J. Appl. Phys. **103**, 083535 (2008); doi: 10.1063/1.2908874
View online: http://dx.doi.org/10.1063/1.2908874
View Table of Contents: http://jap.aip.org/resource/1/JAPIAU/v103/i8
Published by the American Institute of Physics.

Formation mechanisms of ZnO amorphous layers due to thermal treatment of ZnO thin films grown on *p*-InP (100) substrates

J. M. Yuk,[1] J. Y. Lee,[1] Y. S. No,[2] T. W. Kim,[2,a)] and W. K. Choi[3]
[1]*Department of Materials Science and Engineering, Korea Advanced Institute of Science and Technology, Daejeon 305-701, Republic of Korea*
[2]*Division of Electronics and Computer Engineering, Hanyang University, Seoul 133-791, Republic of Korea*
[3]*Thin Film Material Research Center, Korea Institute of Science and Technology, Seoul 136-701, Republic of Korea*

(Received 27 September 2007; accepted 22 February 2008; published online 24 April 2008)

High-resolution transmission electron microscopy (HRTEM) images, selected-area electron diffraction (SAED) patterns, and energy dispersive x-ray spectroscopy (EDS) profiles showed that P atoms accumulated due to thermal treatment on the top sides and in the heterointerface layers of ZnO thin films grown on *p*-InP (100) substrates, resulting in the formation of amorphous ZnO layers in the ZnO thin films. The formation mechanisms of the ZnO amorphous layers due to thermal treatment are described on the basis of the HRTEM, the SAED, and the EDS measurements. © *2008 American Institute of Physics*. [DOI: 10.1063/1.2908874]

I. INTRODUCTION

ZnO thin films have been very attractive because of the interest in investigating both their fundamental physical properties[1–3] and their potential applications in many promising electronic and optoelectronic devices.[4–6] Because ZnO thin films with large energy gaps have unique physical properties of large exciton binding energies and excellent chemical stabilities,[7,8] they have become particularly interesting due to their potential applications in optoelectronic devices, such as light-emitting diodes,[9] photodetectors,[10,11] electroluminescence devices,[12] and ultraviolet (UV) lasers.[13,14] In particular, UV lasers fabricated by utilizing ZnO thin films have emerged as potential candidates for applications in promising next-generation optoelectronic devices operating in the UV region of the spectrum.[15–17] Even though some works concerning ZnO thin films grown on Si substrates have been reported,[3,18–20] very few works have been performed on ZnO thin films grown on III-V compound semiconductor substrates.[21] Even though there are inherent problems due to possible cross-doping effects resulting from interdiffusion or intermixing during growth, ZnO/InP heterostructures have been particularly interesting due to their many possible applications to high-speed optoelectronic and electronic devices. Because thermal treatment is necessary for the fabrication processes of optoelectronic devices fabricated by utilizing ZnO/InP heterostructures, the role of the thermal annealing processes is very important in achieving high-performance devices. Although a few works concerning the physical properties of ZnO/III-V compound semiconductor heterostructures have been reported,[21] very few studies on the formation mechanisms of the amorphous layer due to thermal treatment in ZnO thin films grown on *p*-InP substrates have been reported.

This paper reports the formation mechanisms of ZnO amorphous layers due to thermal treatment in ZnO thin films grown on *p*-InP (100) substrates. Transmission electron microscopy (TEM) measurements were performed to investigate the microstructure of the ZnO/*p*-InP (100) heterostructures. Energy dispersive x-ray spectroscopy (EDS) measurements were carried out to characterize the stoichiometry and the interface quality of the samples. The formation mechanisms of the amorphous layers due to thermal treatment in the ZnO thin films grown on *p*-InP (100) substrates are described on the basis of the high-resolution TEM (HRTEM), the selected-area electron diffraction (SAED), and the EDS results.

II. EXPERIMENTAL DETAILS

Polycrystalline stoichiometric ZnO with a purity of 99.999% was used as a source target material and was precleaned by repeated sublimation. The carrier concentration of the Zn-doped *p*-InP substrates with (100) orientation used in this experiment was 1×10^{16} cm^{-3}. The InP substrates obtained from Sumitomo were alternately degreased in warm acetone and trichloroethylene (TCE) three times, etched in a Br-methanol solution, throughly rinsed in de-ionized water, etched in a mixture of H_2SO_4, H_2O_2, and H_2O (4:1:1) at 40 °C for 10 min, and rinsed in TCE again. After the InP wafers had been chemically cleaned, they were mounted onto a susceptor in a growth chamber. After the chamber had been evacuated to 8×10^{-7} Torr, the deposition was done at a substrate temperature of 200 °C. Ar gas with a purity of 99.999% was used as the sputtering gas. Prior to ZnO growth, the surface of the ZnO target was polished by using Ar^+ sputtering. The ZnO deposition was done at a system pressure of 0.021 Torr and a radio-frequency power (radio frequency of 13.26 MHz) of 100 W. The flow-rate ratio of Ar to O_2 was 2, and the growth rate was approximately 1.17 nm/min. The thermal annealing process was performed in a nitrogen atmosphere with a tungsten-halogen lamp as the

a)Author to whom correspondence should be addressed. Electronic mail: twk@hanyang.ac.kr.

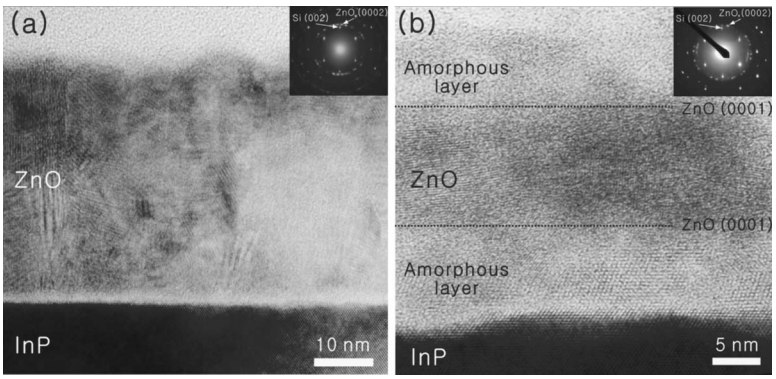

FIG. 1. Cross-sectional high-resolution transmission electron microscopy images of (a) an as-grown ZnO thin film grown on a *p*-InP (100) substrate and of (b) a ZnO thin film grown on a *p*-InP (100) substrate and annealed at 600 °C. The inserts indicate selected-area electron diffraction patterns.

thermal source. The thermal annealing process was carried out for 15 min at temperatures of 500 and 600 °C.

The TEM measurements were performed by using a JEM-ARM1300S transmission electron microscope operating at 1.25 MeV. The samples for the cross-sectional TEM measurements were prepared by cutting and polishing with diamond paper to a thickness of approximately 30 μm and then argon-ion milling at liquid-nitrogen temperature to electron transparency. The energy-dispersive x-ray spectrometer attached to a Tecnai G2 F30 S-Twin system operating at 300 KV was used for EDS.

III. RESULTS AND DISCUSSION

Figure 1 shows cross-sectional HRTEM images of (a) the as-grown ZnO/*p*-InP (100) heterostructure and (b) the heterostructure annealed at 600 °C. The HRTEM image in Fig. 1(a) for the as-grown ZnO/*p*-InP (100) heterostucture shows that the as-grown ZnO thin film had cylindrical columnar structures and a heterointerfacial region with a thickness of about 1 nm between the ZnO thin film and the InP substrate. The corresponding SAED pattern seen in the insert of Fig. 1(a) indicates that the ZnO film has a preferential *c*-axis orientation, giving the lowest surface free energy.[22] The HRTEM image for the ZnO/*p*-InP (100) heterostuctures annealed at 600 °C in Fig. 1(b) shows that the heterostructure contains amorphous layers on the top and the bottom sides of the ZnO thin film. The heterointerfaces between the ZnO thin film and the amorphous layers dominantly appear along the ZnO (0001) planes.

Figure 2 presents the EDS line profiles for an (a) as-grown ZnO/*p*-InP (100) heterostructure and for a (b) heterostructure annealed at 600 °C along the lines on the scanning TEM images in the inserts. Figure 2(a) shows that the heterointerface between the ZnO thin film and the InP substrate for the as-grown sample is relatively abrupt and that the stoichiometry of the grown film is ZnO.[23,24] The EDS line profile for the annealed sample shows that the In atoms have diffused into the bottom side of the ZnO thin film and that the P atoms have accumulated in the amorphous layers on the top and the bottom sides of the ZnO thin film because the surface vapor pressure of In atoms is much lower than that of P atoms at approximately 480 °C.[25,26] The accumulations of P atoms on the ZnO top surface and the ZnO/InP interface layers rather than the middle layers happen because the inflow velocity of P atoms in the ZnO thin film is faster than their diffusion velocity and diffused P atoms accumulate on the end of the ZnO thin films.[27] The formation of the P_{Zn}-$2V_{Zn}$ complex, where P_{Zn} and V_{Zn} are P substitution into the Zn site and the Zn vacancy, respectively, in the top and the bottom sides of the ZnO thin film induces a depletion of Zn atoms in proportion to the accumulation of P atoms.[28,29]

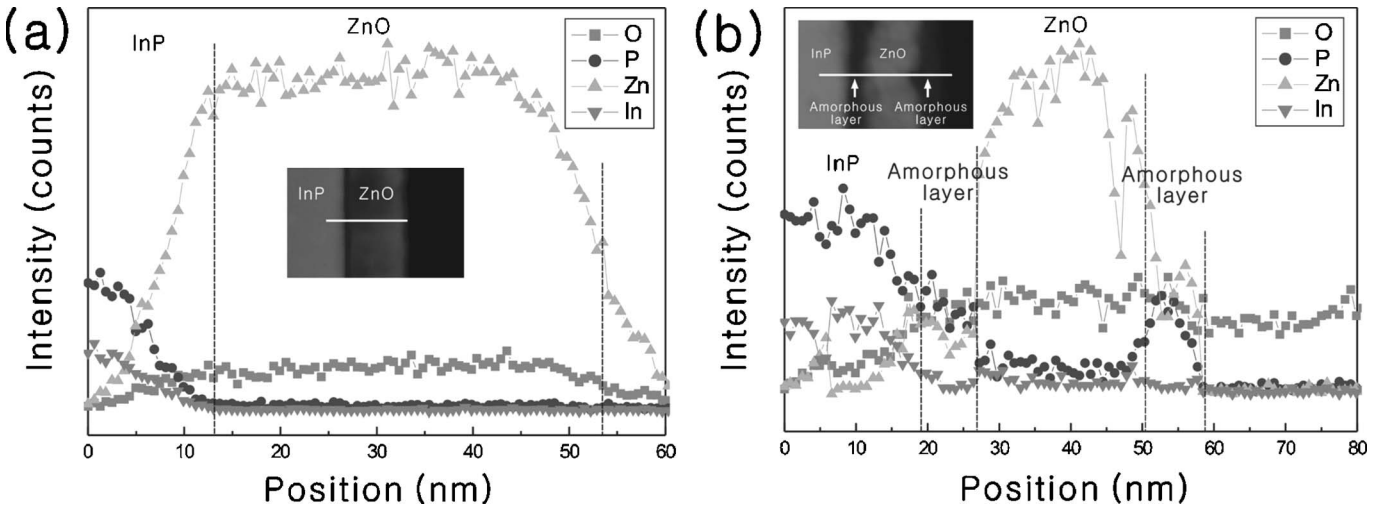

FIG. 2. Energy dispersive x-ray spectroscopy line profiles across the lines shown in the scanning transmission electron microscopy annular dark field images of (a) an as-grown ZnO thin film grown on a *p*-InP (100) substrate and (b) a ZnO thin film grown on a *p*-InP (100) substrate and annealed at 600 °C.

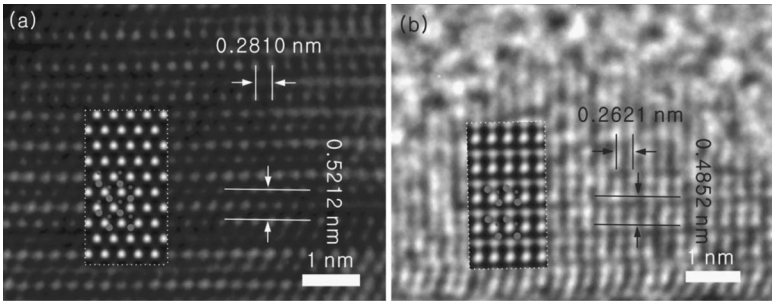

FIG. 3. High-resolution transmission electron microscopy images obtained at the (a) middle and the (b) top regions of the ZnO thin film annealed at 500 °C. The inserts show the proposed model of the layer-by-layer formation of the P_{Zn}-$2V_{Zn}$ complex on the ZnO (0001) planes and a simulated image, as obtained from the NCEMSS software. The red, blue, and green circles indicate Zn, O, and P atoms.

The core P existing in the complex occupies the Zn antisite, which is energetic enough to spontaneously induce two Zn vacancies.[28]

The HRTEM images obtained at the (a) middle and the (b) top of the ZnO thin film annealed at 500 °C, which is almost a starting temperature for surface vaporization of P atoms,[25,26] are shown in Fig. 3. The inserts of Fig. 3 show the proposed models and the simulated results corresponding to the HRTEM images obtained at the middle and the top ZnO layers with perfect stoichiometry and with the layer-by-layer formation of P_{Zn}-$2V_{Zn}$ complexes on ZnO (0001) planes for the ZnO thin film annealed at 500 °C, as constructed by using the NCEMSS software. The atomic spacing distances along the ZnO (0001) and the ZnO $(01\bar{1}0)$ planes of the middle regions of the ZnO films are 0.5212 and 0.2810 nm, respectively, which are in reasonable agreement with those of the ZnO bulk. However, the atomic spacing distances along the ZnO (0001) and the ZnO $(01\bar{1}0)$ planes of the top regions of the ZnO films are 0.4825 and 0.2621 nm, respectively, which are significantly lower due to layer-by-layer formation of P_{Zn}-$2V_{Zn}$ complexes on the ZnO (0001) planes.

Figure 4(a) shows the atomic arrangement of a defect-free section for ZnO bulk materials. The P atoms substitute layer by layer for the Zn atoms on the ZnO (0001) planes on the top and the bottom sides of the ZnO thin film before amorphization of the ZnO thin film. The P_{Zn}-$2V_{Zn}$ complexes are formed from individual defects through the following process:[29]

$$P_{Zn}^{3+} + 2V_{Zn}^{2-} \rightarrow (P_{Zn} - 2V_{Zn})^{-}. \quad (1)$$

An accumulation of Zn vacancy layers on the ZnO (0001) planes might lead to amorphization of the ZnO thin films.[30] Because the Zn vacancy layers are arranged on the ZnO (0001) planes, the heterointerface between the ZnO thin film and the amorphous layer is formed along the ZnO (0001) planes, as shown in Fig. 1(b).

IV. SUMMARY AND CONCLUSIONS

The formation mechanisms of ZnO amorphous layers due to thermal treatment in ZnO thin films grown on *p*-InP (100) substrates were investigated. HRTEM images, SAED patterns, and EDS profiles showed that the P atoms accumulated due to thermal treatment on the top sides and in the heterointerface layers of ZnO thin films grown on *p*-InP (100) substrates, resulting in the formation of Zn vacancies. The accumulation of Zn vacancy layers created an amorphization in the top and the bottom layers of the ZnO thin films due to formation of P_{Zn}-$2V_{Zn}$ complexes.

ACKNOWLEDGMENTS

This work was supported by the Korea Science and Engineering Foundation (KOSEF) grant funded by the Korea government (MOST) (No. R0A-2007-000-20044-0). The authors would like to thank Dr. Youn-Joong Kim at the Korea Basic Science Institute for the use of the high voltage electron microscope.

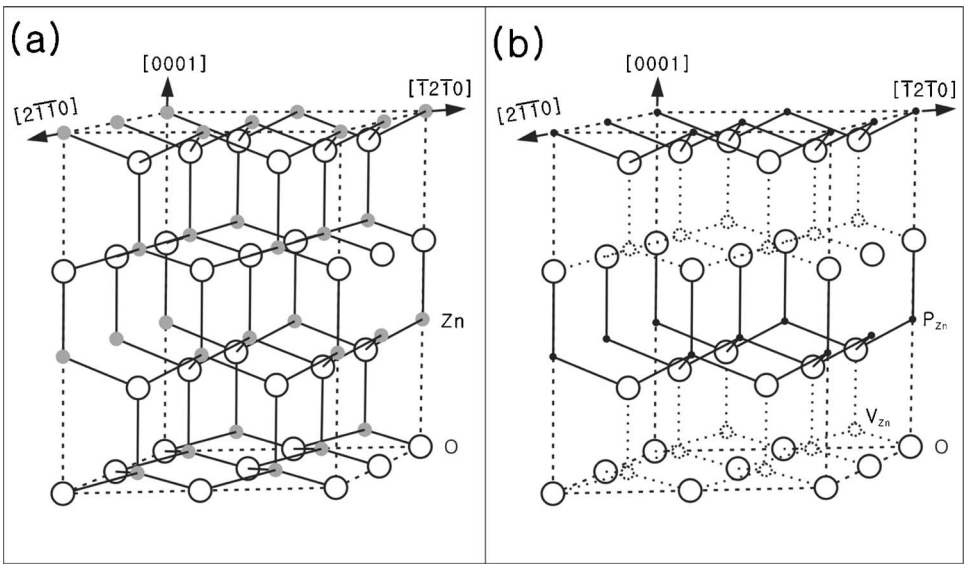

FIG. 4. Atomic arrangements of (a) the defect-free section on ZnO bulk materials for reference and (b) the P_{Zn}-$2V_{Zn}$ complexes on the top and the bottom layers of the ZnO thin films grown on *p*-InP (100) substrates and annealed at 600 °C. The dashed bonds shown in (b) indicate the broken O–Zn bonds relative to the ZnO bulk materials.

[1]J. Zúñiga-Pérez, V. Muñoz-Sanjosé, E. Palacios-Lidón, and J. Colchero, Phys. Rev. Lett. **95**, 226106 (2005).
[2]Y. J. Zeng, Z. Z. Ye, J. G. Lu, W. Z. Xu, L. P. Zhu, B. H. Zhao, and S. Limpijumnong, Appl. Phys. Lett. **89**, 042106 (2006).
[3]J. W. Shin, J. Y. Lee, Y. S. No, T. W. Kim, and W. K. Choi, Appl. Phys. Lett. **89**, 101904 (2006).
[4]R. F. Service, Science **276**, 895 (1997).
[5]A. Tsukazaki, A. Ohtomo, T. Onuma, M. Ohtani, T. Makino, M. Sumiya, K. Ohtani, S. F. Chichibu, S. Fuke, Y. Segawa, H. Ohno, H. Koinuma, and M. Kawasaki, Nat. Mater. **4**, 42 (2005).
[6]T. Moe Borseth, B. G. Svensson, and A. Yu. Kuznetsov, Appl. Phys. Lett. **89**, 262112 (2006).
[7]T. Soki, Y. Hatanaka, and D. C. Look, Appl. Phys. Lett. **76**, 3257 (2000).
[8]F.-Y. Jen, Y.-C. Lu, C.-Y. Chen, H.-C. Wang, and C. C. Yang, Appl. Phys. Lett. **87**, 252117 (2005).
[9]M. S. Gudiksen, L. J. Lauhon, J. Wang, D. C. Smith, and C. M. Lieber, Nature (London) **415**, 617 (2002).
[10]H. Kind, H. Q. Yan, B. Messer, M. Law, and P. D. Yang, Adv. Mater. (Weinheim, Ger.) **14**, 158 (2002).
[11]Z. Y. Fan, P. C. Chang, J. G. Lu, E. C. Walter, R. M. Penner, C.-H. Lin, and H. P. Lee, Appl. Phys. Lett. **85**, 6128 (2004).
[12]W. I. Park and G. C. Yi, Adv. Mater. (Weinheim, Ger.) **16**, 87 (2004).
[13]P. D. Yang, H. Q. Yan, S. Mao, R. Richard, J. Justin, S. Richard, M. Nathan, P. Johnny, R. He, and H. J. Choi, Adv. Funct. Mater. **12**, 323 (2002).
[14]J. C. Johnson, H. Q. Yan, P. D. Yang, and R. J. Saykally, J. Phys. Chem. B **107**, 8816 (2003).
[15]Z. K. Tang, G. K. L. Wong, P. Yu, M. Kawasaki, A. Ohtomo, H. Koinuma, and Y. Segawa, Appl. Phys. Lett. **72**, 3270 (1998).
[16]S. F. Yu, C. Yuen, S. P. Lau, and H. W. Lee, Appl. Phys. Lett. **84**, 3244 (2004).
[17]H. D. Li, S. F. Yu, A. P. Abiyasa, C. Yuen, S. P. Lau, H. Y. Yang, and E. S. P. Leong, Appl. Phys. Lett. **86**, 261111 (2005).
[18]K. Ogata, S.-W. Kim, Sz. Fujita, and Sg. Fujita, J. Cryst. Growth **240**, 112 (2002).
[19]Y. L. Liu, Y. C. Liu, Y. X. Liu, D. Z. Shen, Y. M. Lu, J. Y. Zhang, and X. W. Fan, Physica B **322**, 31 (2002).
[20]J. M. Yuk, J. Y. Lee, J. H. Jung, T. W. Kim, D. I. Son, and W. K. Choi, Appl. Phys. Lett. **90**, 031907 (2007).
[21]M. K. Ryu, S. H. Lee, M. S. Jang, G. N. Panin, and T. W. Kang, J. Appl. Phys. **92**, 154 (2002).
[22]N. Fujimura, T. Nishhara, S. Goto, J. Xua, and T. Ito, J. Cryst. Growth **130**, 269 (1993).
[23]L. Wang, T. Y. Chen, C. L. Chien, and C. Leighton, Appl. Phys. Lett. **88**, 232509 (2006).
[24]A. R. Kortan, R. Hull, R. L. Opila, M. G. Bawendi, M. L. Steigerwald, P. J. Carroll, and L. E. Brus, J. Am. Chem. Soc. **112**, 1327 (1990).
[25]S. J. Chen, Y. C. Liu, C. L. Shao, Y. M. Lu, J. Y. Zhang, D. Z. Shen, and X. W. Fan, Chem. Phys. Lett. **397**, 360 (2004).
[26]F. Riesz, L. Dobos, C. Vignali, and C. Pelosi, Mater. Sci. Eng., B **80**, 54 (2001).
[27]M. H. Badawi, B. J. Sealy, and K. G. Stephens, J. Phys. D: Appl. Phys. **15**, 507 (1982).
[28]S. Limpijumnong, S. B. Zhang, S.-H. Wei, and C. H. Park, Phys. Rev. Lett. **92**, 155504 (2004).
[29]W. J. Lee, J. G. Kang, and K. J. Chang, Phys. Rev. B **73**, 024117 (2006).
[30]A. I. Titov and S. O. Kucheyev, Nucl. Instrum. Methods Phys. Res. B **168**, 375 (2000).